19th Australasian Fluid Mechanics Conference
Melbourne, Australia
8-11 December 2014

Heat Transfer Augmentation using Rectangular Cross-Section Turbulence Generators in Confined Quasi-Two-Dimensional Magneto-Hydrodynamic Flows

O.G.W. Cassells, W.K. Hussam and G.J. Sheard

Department of Mechanical and Aerospace Engineering
Monash University, Victoria 3800, Australia

Abstract

Heat transfer efficiency from a duct side-wall in which an electrically conducting fluid flows under the influence of a transverse magnetic field is investigated in the present work. The study intends to provide useful guidelines to improve efficiency of MHD cooling systems while also taking into account that practical designs should be both thermally efficient and inexpensive in terms of pumping power. A quasi-two-dimensional MHD model is employed to model the flow using high-resolution direct numerical simulation. The gap height, incidence angle and spacing ratio of rectangular cylinders with aspect ratio $\alpha = 1/2$ and blockage ratio $\beta = 1/4$ are independently varied to establish optimal configurations determined by an efficiency index; the ratio of heat transfer enhancement to pressure drop penalty. At gap heights between 2 and 1.5 cylinder lengths L_c from the heated duct wall it was found that 95% of the peak heat transfer efficiency can be achieved. Furthermore, cylinders offset at a gap height of $G = 1.5L_c$ experienced no additional efficiency benefits from cylinder inclination. However, cylinders placed at the duct centreline received improved thermal efficiency for $-15^\circ \leq \gamma \leq 30^\circ$. For upright tandem configurations at a gap height of $G = 1.5L_c$, peak efficiency $\eta_{\text{eff}} = 1.317$ and heat transfer $HR = 2.541$ occurred at spacings of $(S-h_c)/L_c = 6$ and $(S-h_c)/L_c = 8$, respectively.

Introduction

Magneto-hydrodynamic (MHD) duct flow in the presence of a transverse magnetic field occurs within the liquid metal cooling blankets surrounding magnetically confined fusion reactor plasma. Liquid metals moving under the influence of uniform magnetic fields are subjected to electromagnetic 'Lorentz' forces due to interactions with motion-induced electric currents [1]. Research on such flows has shown that for sufficiently strong transverse magnetic fields, velocity differentials in perpendicular planes are strongly suppressed, while propagation vortices also become elongated and aligned with the magnetic field [1]. Duct walls normal to the magnetic field are subjected to the formation of boundary layers known as Hartmann layers which exert frictional forces on the internal core flow. Hence, a quasi-two-dimensional model can be constructed to investigate these flows by augmenting the two-dimensional Navier–Stokes equations with additional forcing and linear braking terms representing the Lorentz forces and friction in the Hartmann layers, respectively [2].

Due to the dampening of velocity fluctuations along the direction of the magnetic field, longitudinal vortices are dissipated rapidly and thus, transverse vortex generation is considered the only viable vortex orientation for heat transfer enhancement in duct MHD flows [3]. Heat transfer enhancement using internal obstacles to induce transverse vortices has been the subject of investigation for both MHD and hydrodynamic flows. It has been established that there is an optimal gap height above a heated wall at which heat transfer efficiency is maximised. At this height wake vortices are cast close enough to the heated wall to enhance mixing between low and high temperature fluids, but are still high enough to prevent vortex suppression [4]. Research into obstacles with aspect ratio $\alpha = h_c/L_c = 1/2$ and blockage ratio $\beta = L_c/h = 1/3$ at angles of attack $-45^\circ \leq \gamma \leq 45^\circ$ in low Re two-dimensional flows has shown that potential heat transfer improvements of over 50% could be achieved without significant pressure drop penalties [5]. Numerical investigations into tandem configurations have also highlighted that potential increases in heat transfer from heated sidewalls of up to 78% can be achieved at spacing ratios of $S/h = 2,3,4$ [6]. In addition, it has been shown that the spacing ratio of tandem configurations can significantly affect the pressure drop characteristics of unsteady two-dimensional channel flows [7]. It is therefore expected that there is some finite gap ratio, incidence angle and spacing ratio that maximise the heat transfer efficiency for quasi-two-dimensional MHD duct flow.

The present work aims to identify the optimal heat transfer efficiency configurations by varying gap height, incidence angle, and spacing ratio of rectangular turbulence generators with $\alpha = 1/2$ and $\beta = 1/4$ in quasi-two-dimensional MHD duct flow for $Re = 2000$ and $Ha = 100$.

Problem Definition

The system proposed for analysis is shown in figure 1. A long rectangular duct of height h and length L confines electrically and thermally insulated rectangular cylinders of aspect ratio $\alpha = h_c/L_c = 1/2$ and blockage ratio $\beta = L_c/h = 1/4$ orientated with their axis perpendicular to the flow direction. The electrically insulated upper and lower duct walls are kept at representative cold and hot temperatures T_o and T_w, respectively. A homogenous magnetic field of magnitude B acts parallel to the cylinder axis. The upstream and downstream lengths in relation to the first turbulence generator centroid are $x_u = 15L_c$ and $x_d = 50L_c$, respectively. The effect of gap height G of a single upright cylinder for $0.8L_c \leq G \leq 1.5L_c$ on heat transfer efficiency is firstly considered. The influence of cylinder incidence angle γ on heat transfer efficiency at both the optimal gap height and duct centreline is considered for $-45^\circ \leq \gamma \leq 45^\circ$. Tandem configuration spacing ratios are varied for $(S-h_c)/L_c$ = 1 ,2 ,4 ,6, 8 at the optimal heat transfer efficiency gap height for the optimal angle of attack case. For each parameter investigation, a Hartmann Number $Ha = 100$ and Reynolds number $Re = 2000$ will be considered to maintain consistency with practical limitations, exhibit unstable flow behaviour, and meet the validity conditions of the quasi-two-dimensional MHD model proposed by Sommeria and Moreau [1]. A Prandtl number of $\text{Pr} = 0.022$ is used to be representative of eutectic alloy GaInSn.

Mathematical Formulation

For sufficiently high Hartmann numbers, the ratio of flow induced to applied magnetic field, represented by the magnetic Reynolds number Re_m, is very small. Therefore, it is sufficient to consider the applied magnetic field in the out-of-plane di-

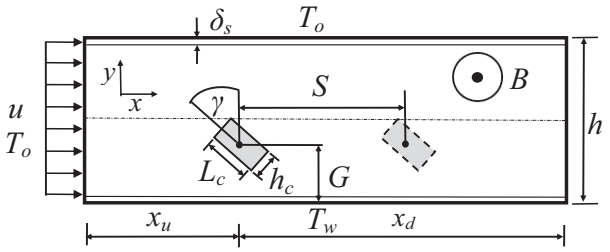

Figure 1. Schematic diagram of the flow configuration and parameters used in the present study. Here, δ_s is the thickness of the sidewall boundary layer known as Shercliff layers.

rection only. The quasi-two-dimensional model for the present configuration is adapted from that derived by Sommeria and Moreau and Pothérat et al [1, 2]. Here, parameter scaling is consistent with that used by Hussam and Sheard such that lengths are scaled by the cylinder length L_c, pressure by ρU_0^2 where ρ is the density and U_0 is the peak inlet velocity, time by L_c/U_0, and temperature by the imposed temperature difference between the duct side-walls, ΔT [4]. Hence, the dimensionless continuity, momentum, and energy MHD equations can be expressed as

$$\nabla \cdot \mathbf{u} = 0, \tag{1}$$

$$\frac{\partial \mathbf{u}}{\partial t} + (\mathbf{u}\cdot\nabla)\mathbf{u} + \nabla p = \frac{1}{Re}\nabla^2\mathbf{u} - 2\left(\frac{L_c}{a}\right)^2 \frac{Ha}{Re}\mathbf{u}, \tag{2}$$

$$\frac{\partial T}{\partial t} + (\mathbf{u}\cdot\nabla)T = \frac{1}{Pe}\nabla^2 T, \tag{3}$$

where $\mathbf{u}$, p and T are the velocity, kinematic pressure, and temperature fields, respectively, projected onto the x-y plane. The dimensionless parameters, Reynolds number, Hartmann number and Péclet number, are respectively defined as

$$Re = \frac{U_0 L_c}{\nu}, \tag{4}$$

$$Ha = aB\sqrt{\frac{\sigma}{\rho\nu}}, \tag{5}$$

$$Pe = Re\,Pr, \tag{6}$$

ν, σ, and a are the kinematic viscosity, magnetic permeability of the liquid metal, and half the out-of-plane duct height, respectively. The Prandtl number $Pr = \nu/k_T$, where k_T is the thermal diffusivity of the fluid.

The efficiency index of heat transfer augmentation is given by the ratio of heat transfer enhancement to pressure drop penalty

$$\eta_{\text{eff}} = \frac{HR}{PR}, \tag{7}$$

where HR and PR are the heat transfer enhancement and the pressure drop penalty ratios, respectively. HR and PR are given by

$$HR = \frac{Nu}{Nu_0}, \tag{8}$$

$$PR = \frac{\Delta P}{\Delta P_0}. \tag{9}$$

Nu and ΔP are the local time averaged Nusselt number on the lower wall and total pressure drop across the duct length for the augmented cases, respectively. The subscript 0 denotes the empty duct reference case.

Numerical Methodology

A high order spectral element method is employed to discretise the governing equations. A no-slip boundary condition is applied on all solid surfaces and the channel inlet flow conditions are composed of the analytical solution for fully developed quasi-two-dimensional free flow [8]. Standard spectral element solver outflow boundary conditions of constant reference pressure Dirichlet, and a zero out of plane velocity gradient Neumann conditions are imposed at the duct exit. A high order Neumann pressure gradient condition is also applied to the other boundaries to maintain third order time accuracy [9]. The domain is meshed using a series of macro-elements with internally applied Langrangian polynomial mapping functions. A graded element distribution is employed along solid surfaces to help resolve regions that undergo large gradients such as flow separation at cylinder corners and shear within boundary layers.

A grid resolution study was conducted to ensure adequate spatial and temporal sampling to accurately resolve the dynamics of the flow field. Both $h-$ and $p-$ refinement were employed to measure the convergence of the domain size and resolution sensitive heat flux ϕ, pressure and viscous drag C_{dp} and C_{dv}, lift C_l, and L_2 norm parameters. The grid resolution study was conducted by refining the polynomial mapping function over $4 \leq N \leq 9$. The $\gamma = 0^\circ$ and $\gamma = 45^\circ$ cases were investigated to represent the extremes of expected flow complexity. Due to spatial under-sampling of the thermal boundary layers, additional h-refinement of the mesh size in regions adjoining the duct walls was utilised to obtain better convergence of absolute heat flux. Physical irregularities in the shedding of vortices led to asymmetry in advection of the wake vortices downstream. Although a general trend of convergence was obtained, the asymmetry in vortex streets led to non-monotonic convergence over the polynomial range tested. However, for the chosen polynomial order of $N = 8$, a convergence of better than 1.03% for all representative parameters was obtained.

Results and Discussion

Gap Height

The HR, PR, η_{eff} response to cylinder gap height variation above the heated wall is shown in figure 2. A peak in overall heat transfer efficiency of 42.6% occurs for $G/L_c \approx 1.5$, with 95% of this efficiency being achieved in the range $1.5 \leq G/L_c \leq 2$. These findings support those discussed in the introduction with respect to a critical gap height at which heat transfer enhancement can be optimised without significant pressure drop penalties. In regions approaching the duct walls, vorticity suppression coupled with a region of retarded flow cause a reduction in viscous dissipation and thermal mixing; and in turn a decrease in HR and PR. Viscous stresses created by the shearing between fluid elements and solid boundaries lead to energy dissipation in the flow. Hence, increased vorticity magnitudes, characterised by a decrease in scale, are less beneficial to heat transport and can lead to an increase in pressure drops losses due to viscous dissipation. The pressure drop characteristics are qualitatively symmetric about the centreline due to spatial symmetry in the domain.

It is important to note, the peak HR increase of 206% occurring for $G/L_c = 1.675$ indicates that the best configuration from an efficiency standpoint is not necessarily the one with the largest heat transfer enhancement if it comes at a cost of higher mechanical losses. As highlighted in the vorticity and temperature field plots for $G/L_c = 1.5$ in figure 3, the vortices

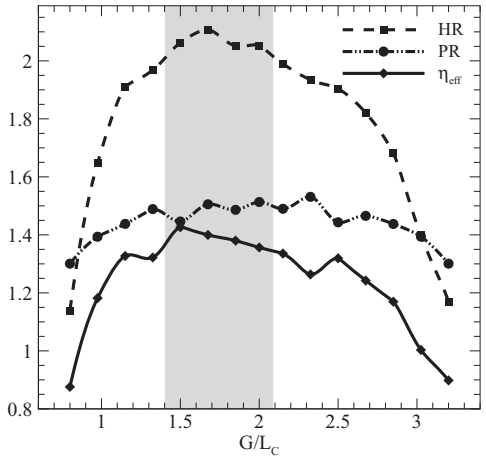

Figure 2. Variation of *HR*, *PR*, and η_{eff} for $Re = 2000$, $Ha = 100$,and $\gamma = 0^\circ$ for $0.8L_c \leq G \leq 1.5L_c$. The shaded region highlights where η_{eff} is within 95% of its peak value.

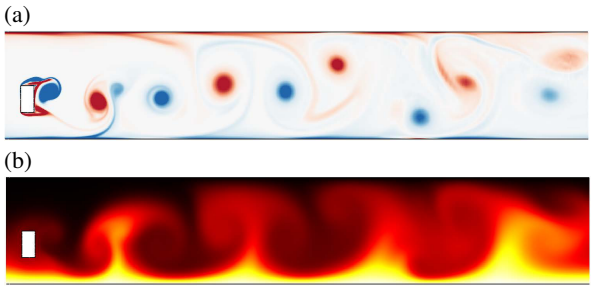

Figure 3. Vorticity (a) and dimensionless temperature (b) contours for $Re = 2000$, $Ha = 100$, $G/L_c = 1.5$ and $\gamma = 0^\circ$. Blue and red contours represent negative and positive vorticity, respectively. Red and black contours represent warmer and colder temperatures, respectively.

shed from the lower cylinder surface interact efficiently with the bottom thermal boundary layer; leading to a larger transport of high temperature fluid away from the wall without excessive viscous dissipation.

Incidence Angle

The response curves of *HR*, *PR* and η_{eff} for $-45^\circ \leq \gamma \leq 45^\circ$ at $G/L_c = 1.5$ and $G/L_c = 2$ are shown in figures 4 and 5, respectively. At $G/L_c = 1.5$ a peak in η_{eff} of 42.6% is achieved at $\gamma = 0^\circ$ and a maximum *HR* of 207% occurs for $\gamma = -30^\circ$. Benefits to overall heat transfer efficiency were not achieved even though heat transfer enhancement was slightly aided through obstacle inclination. For $0^\circ \leq |\gamma| \leq 15^\circ$ a slight decrease in *HR*, *PR* and η_{eff} is observed. The changes in *HR* and η_{eff} are more pronounced for positive incidence angles due to spatial asymmetry at this gap height. For $15^\circ \leq |\gamma| \leq 30^\circ$, there is a clear increase in *HR* and η_{eff}. However, an increase in *PR* is only observed for negative angles as the wake vorticity is shed towards the lower wall causing a larger rate of viscous dissipation. For $|\gamma| > 30^\circ$, the trend is reversed with decreasing *HR*, *PR* and η_{eff}. For $-37.5^\circ \leq \gamma \leq 7.5^\circ$ and $25^\circ \leq \gamma \leq 35^\circ$, 95% of the peak η_{eff} can be achieved. It should be noted that a contributing factor to the overall pressure drop reductions for increased incidence angles is the effective reduction in blockage ratio.

When the cylinder is located at the duct centreline, a peak of $\eta_{\text{eff}} = 1.412$ is observed for $\gamma = 15^\circ$. This corresponds to a 4.2% improvement in efficiency over the upright orientation. 98% of

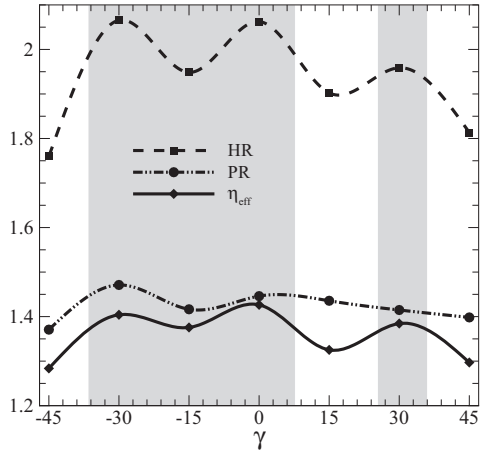

Figure 4. Variation of *HR*, *PR*, and η_{eff} for $Re = 2000$, $Ha = 100$, $G/L_c = 1.5$, and $-45^\circ \leq \gamma \leq 45^\circ$. The shaded region highlights where η_{eff} is within 95% of its peak value.

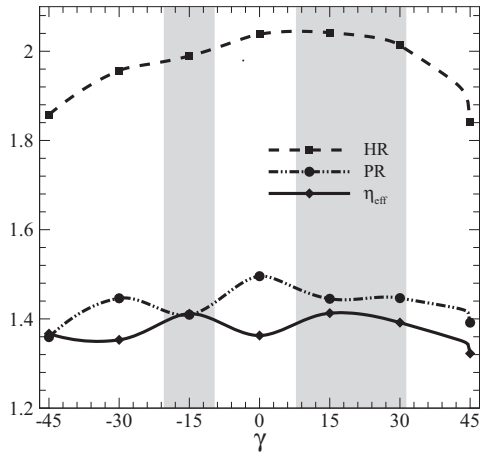

Figure 5. Variation of *HR*, *PR*, and η_{eff} for $Re = 2000$, $Ha = 100$, $G/L_c = 2$, and $-45^\circ \leq \gamma \leq 45^\circ$. The shaded region highlights where η_{eff} is within 98% of its peak value.

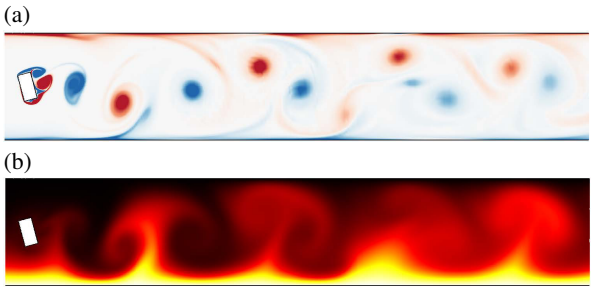

Figure 6. Vorticity (a) and dimensionless temperature (b) contours for $Re = 2000$, $Ha = 100$, $G/L_c = 2$ and $\gamma = 15^\circ$. Blue and red vorticity contours represent negative and positive rotations, respectively. Red and black temperature contours represent warmer and colder temperatures, respectively.

the peak η_{eff} can be achieved in the ranges of $7.5^\circ \leq \gamma \leq 30^\circ$ and $-10^\circ \leq \gamma \leq -20^\circ$. Significant increases in *PR* between data points is only observed for negative incidence angles, which is consistent with the behaviour observed for the $G/L_c = 1.5$ case. As most readily seen in figure 6, counter clockwise rotating vor-

tices shed from the lower cylinder surface interact efficiently with the heated side-wall thermal boundary layer, creating large plumes of high temperature fluid upwards. A maximum *HR* of 205% is observed for $\gamma = 0^\circ$. As with previous results, a peak in *HR* did not correspond to the most efficient heat transfer enhancement configuration.

Spacing Ratio of Tandem Cylinders

The response of *HR*, *PR*, and η_{eff} for varying upright cylinder spacing ratio $(S-h_c)/L_c = 1,2,4,6,8$ offset at $G/L_c = 1.5$ is shown in Figure 7. A monotonic increase in *HR* and *PR* is observed for increasing spacing ratios due to promoted mixing and viscosity driven energy dissipation from amplified chaotic fluctuations. Heat transfer enhancement from the lower wall follows an approximate logarithmic relationship, with a peak of $HR = 245\%$ occuring at $(S-h_c)/L_c = 8$. This is accompanied by a sharp increase in *PR* due to the vortex wake advecting upwards through the inter-cylinder gap and interacting with the top wall boundary layer. A maximum efficiency of $\eta_{\text{eff}} = 1.317$ was achieved at $(S-h_c)/L_c = 6$. The peak efficiency spacing ratio corresponds to obstacle locations at which the Karman vortex sheets shed from the upstream cylinder can travel through the inter-cylinder gap unimpeded. This is most readily seen from the vorticity and temperature contour plots shown in figure 8. The downstream cylinder acts to re-energise the flow by creating new larger scale vorticity which promotes thermal mixing.

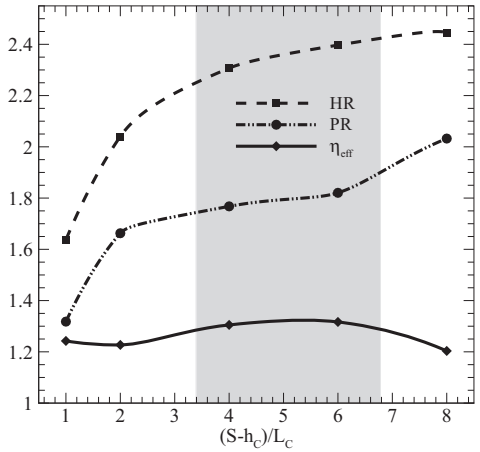

Figure 7. Variation of *HR*, *PR*, and η_{eff} for $Re = 2000$, $Ha = 100$, $G/L_c = 1.5$, $\gamma = 0^\circ$ and $1 \leq (S-h_c)/L_c \leq 8$. The shaded region highlights where η_{eff} is within 98% of its peak value.

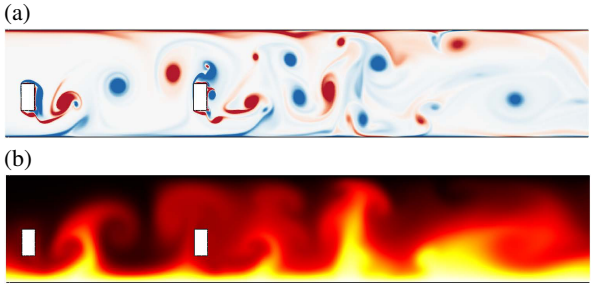

Figure 8. Vorticity (a) and dimensionless temperature (b) contours for $G/L_c = 1.5$, $(S-h_c)/L_c = 6$ and $\gamma = 0^\circ$. Blue and red contours represent negative and positive vorticity, respectively. Red and black contours represent warmer and colder temperatures, respectively

Conclusion

The present study numerically investigated the heat transfer and pressure drop characteristics of confined liquid metal flow under a strong axial magnetic field past a rectangular cylinder at varying gap height, incidence angle and tandem configuration spacing ratio. Heat transfer efficiency was found to be higher for a single cylinder offset from the duct centreline with gap height ratio $1.5 \leq G/L_c \leq 2$. No additional heat transfer efficiency improvements were obtained by inclining the cylinder when offset at $G/L_c = 1.5$. However, for a cylinder placed at the duct centreline, thermal efficiency peaked at $\gamma = 15^\circ$, with a 41% efficiency improvement over the empty channel case, and a 4% improvement over an upright cylinder. Tandem cylinders offset from the centreline achieved a 32% increase in η_{eff} for $(S-h_c)/L_c = 6$, and a 254% improvement in *HR* at $(S-h_c)/L_c = 8$ when compared to an empty channel.

Acknowledgements

This research was supported by ARC Discovery Grant DP120100153, high-performance computing time allocations from the National Computational Infrastructure (NCI) and the Victorian Life Sciences Computation Initiative (VLSCI), and the Monash SunGRID.

References

[1] Sommeria, J. and Moreau, R., Why, how, and when, mhd turbulence becomes two-dimensional, *Journal of Fluid Mechanics*, **118**, 1982, 507–518.

[2] Pothérat, A., Sommeria, J. and Moreau, R., An effective two-dimensional model for mhd flows with transverse magnetic field, *Journal of Fluid Mechanics*, **424**, 2000, 75–100.

[3] Mück, B., Günther, C., Müller, U. and Bühler, L., Three-dimensional mhd flows in rectangular ducts with internal obstacles, *Journal of Fluid Mechanics*, **418**, 2000, 265–295.

[4] Hussam, W. K. and Sheard, G. J., Heat transfer in a high hartmann number mhd duct flow with a circular cylinder placed near the heated side-wall, *International Journal of Heat and Mass Transfer*, **67**, 2013, 944–954.

[5] Meis, M., Varas, F., Velázquez, A. and Vega, J. M., Heat transfer enhancement in micro-channels caused by vortex promoters, *International Journal of Heat and Mass Transfer*, **53**, 2010, 29–40.

[6] Valencia, A., Numerical study of self-sustained oscillatory flows and heat transfer in channels with a tandem of transverse vortex generators, *Heat and Mass Transfer*, **33**, 1998, 465–470.

[7] Daloglu, A., Pressure drop in a channel with cylinders in tandem arrangement, *International Communications in Heat and Mass Transfer*, **35**, 2008, 76–83.

[8] Dousset, V. and Pothérat, A., Numerical simulations of a cylinder wake under a strong axial magnetic field, *Physics of Fluids (1994-present)*, **20**, 2008, –.

[9] Karniadakis, George Em., Israeli, Moshe. and Orszag, Steven A., High-order splitting methods for the incompressible Navier-Stokes equations, *Journal of Computational Physics*, **97**, 1991, 414–443.